Supporting Information

Lu et al. 10.1073/pnas.1319138111

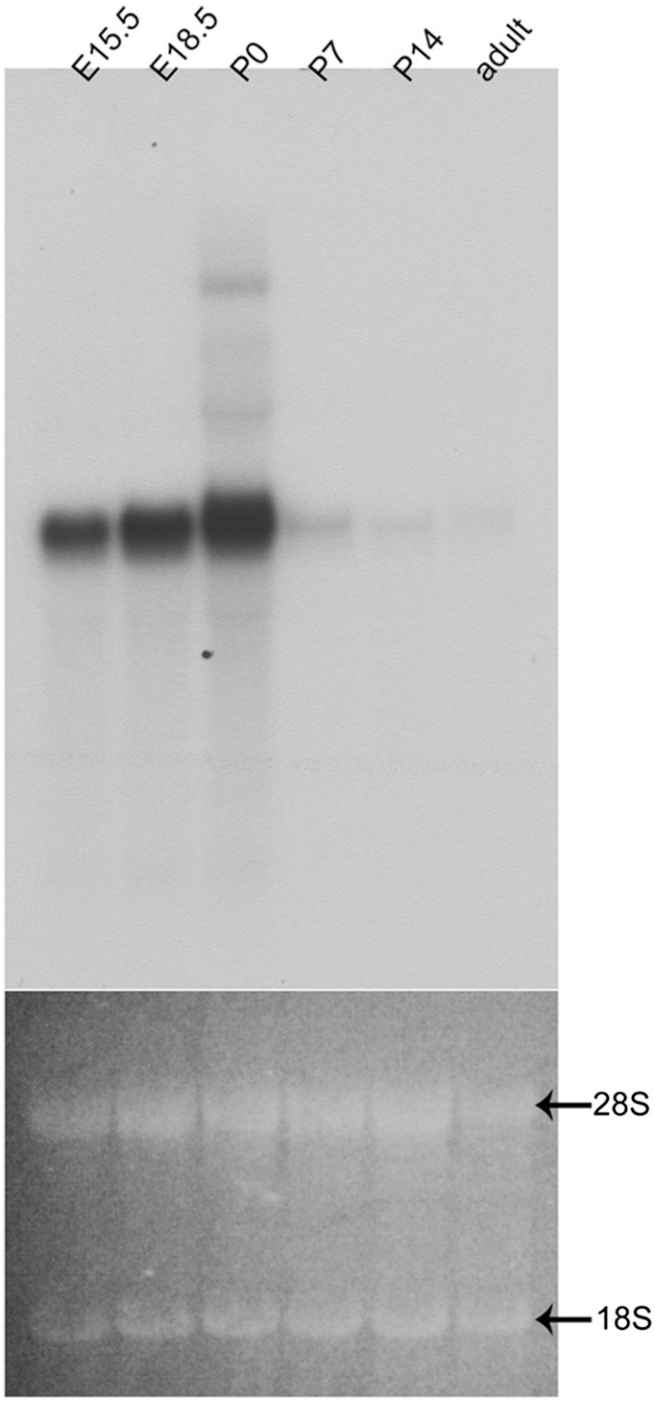

Fig. S1. Developmental expression profile of striatal *Isl1* mRNA. (*Upper*) Northern blotting shows that *Isl1* mRNA is progressively expressed at a high level in the striatum from embryonic day (E) 15.5 to postnatal day (P) 0. *Isl1* mRNA is dramatically reduced at P7, P14, and adulthood (black bands). (*Lower*) Ribosomal RNA of loading controls (28S, 18S) is shown (arrows).

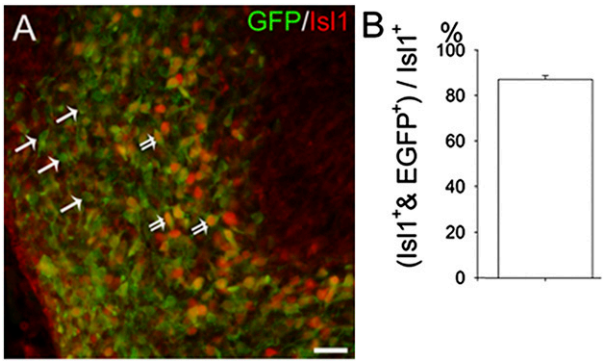

Fig. S2. Recombination efficiency of Isl1-Cre activity in the *Isl1-Cre;CAG-CAT-EGFP* brain at E12.5. (*A* and *B*) Cre recombination efficiency in *Isl1-Cre* mice is assayed by intercrossing *Isl1-Cre* mice with *CAG-CAT-EGFP* reporter mice. Double immunostaining of Isl1 (red) and EGFP (green) proteins shows that about 87% of Isl1$^+$ cells coexpress recombinated EGFP (double arrows). Some Isl1$^+$ cells without EGFP signals are observed (*A*, arrows), which may represent down-regulation of Isl1 in Isl1$^+$ progeny. $n = 3$. (Scale bar: 50 μm.)

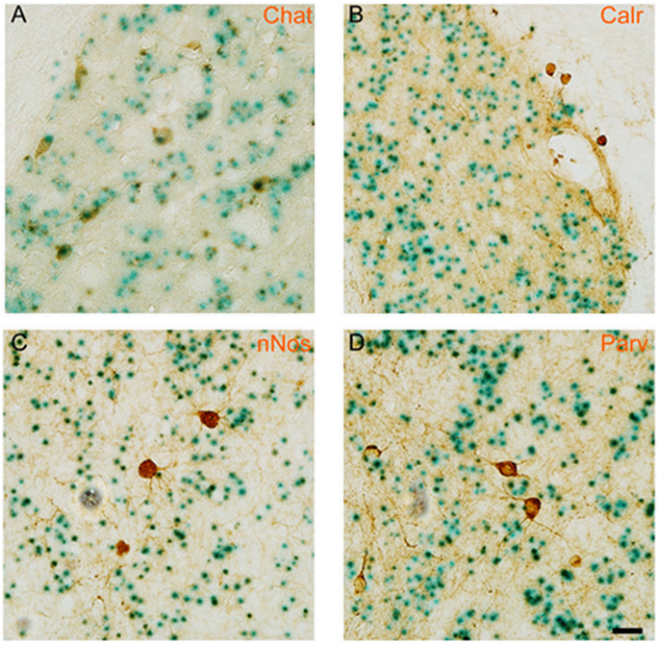

Fig. S3. Isl1 cell lineages develop into striatal cholinergic interneurons, but not other types of striatal interneurons. (*A*) In P25 striatum of *Isl1-Cre;Rosa26R* mice, most choline acetyltransferase (ChAT)-immunoreactive cholinergic interneurons are found to contain β-gal signals. None or, at most, a few calretinin$^+$ (Calr) (*B*), neuronal Nos$^+$ (nNos) (*C*), and parvalbumin$^+$ (Parv) (*D*) interneurons coexpress β-gal. (Scale bar: 25 μm.)

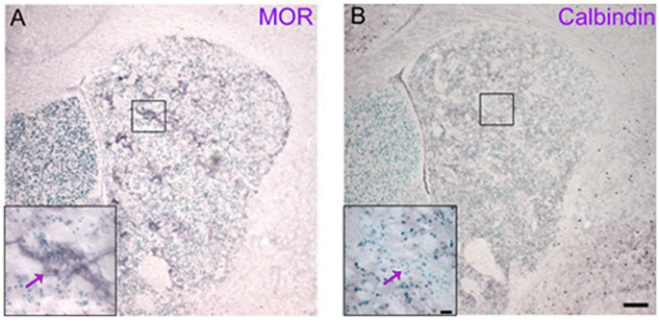

Fig. S4. Isl1$^+$ progeny are present in both striosomal and matrix compartments. In P25 striatum of *Isl1-Cre;Rosa26R* mice, β-gal$^+$ cells are localized in mu-opioid receptor (MOR)-positive [*A* (*Inset*, purple arrow)] and calbindin-poor striosomes [*B* (*Inset*, purple arrow)]. (*B*) β-gal$^+$ cells are also localized in calbindin-rich matrix. (*Insets*) Boxed regions in *A* and *B* are shown at high magnification. (Scale bars: *A* and *B*, 200 μm; *Insets*, 25 μm.)

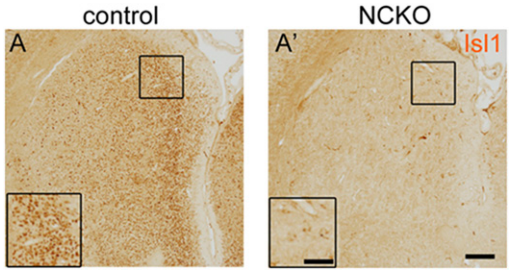

Fig. S5. Loss of striatal Isl1 expression in the *Nestin-Cre;Isl1*$^{f/f}$ brains. (*A*) High levels of Isl1 immunoreactivity are present in the medial control striatum of *Nestin-Cre;Isl1*$^{fl/+}$ brain at E18.5. (*A′*) Isl1 immunoreactivity is absent in the mutant striatum of *Nestin-Cre;Isl1*$^{f/f}$ brain. (*Insets*) Boxed regions in *A* and *A′* are shown at high magnification. (Scale bars: *A* and *A′*, 100 μm; *Insets*, 50 μm.)

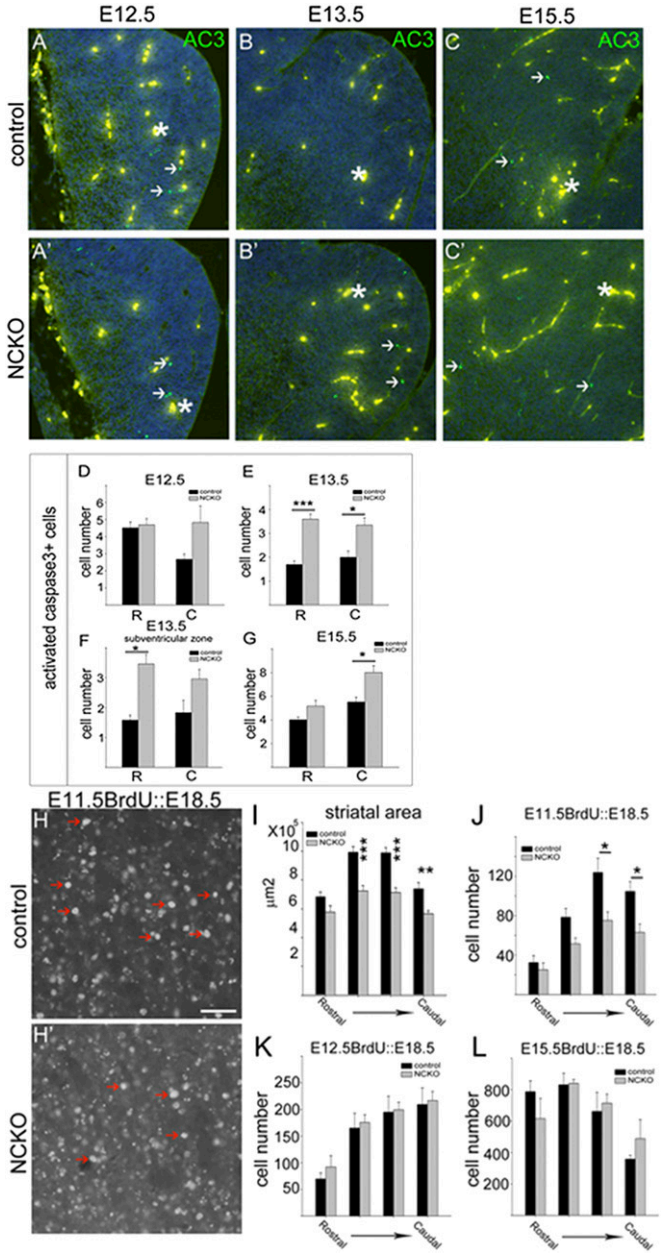

Fig. S6. Abnormal apoptosis in *Isl1* mutant striatum at early embryonic stages. (*A*, *A′*, and *D*) Immunostaining shows that activated caspase 3$^+$ (AC3$^+$) cells are present in *Nestin-Cre;Isl1$^{f/f}$* (ncKO) striatum at E12.5. (*B*, *B′*, *E*, and *F*) Significant increases of AC3$^+$ cells are detected in *Isl1* mutant striatum at E13.5. (*B*, *B′*, and *F*) Note that AC3$^+$ cells are primarily detected in the subventricular zone (*B′*, arrows). (*C*, *C′*, and *G*) By E15.5, increases of AC3$^+$ cells are also found in the caudal mutant striatum. (*A*–*C′*) Nonspecific vascular staining is indicated by asterisks. (*H*, *H′*, and *J*) Decreases of strong BrdU$^{E11.5}$-labeled cells in the caudal E18.5 mutant striatum (*H* and *H′*, arrows). No significant changes of strong BrdU$^{E12.5}$-labeled (*K*) and BrdU$^{E15.5}$-labeled (*L*) cells are found in E18.5 mutant striatum. (*I*) Reduction of striatal areas is observed in E18.5 mutant brain. *$P < 0.05$; **$P < 0.01$; ***$P < 0.001$. AC3$^+$ in E12.5, E13.5, and E15.5 (*D*–*G*), $n = 3$; BrdU$^{E11.5}$-, BrdU$^{E12.5}$-, and BrdU$^{E15.5}$-labeled cells (*J*–*L*), $n = 3$; and striatal area (*I*), $n = 9$. (Scale bar: *A*–*C′*, *H*, and *H′*, 50 μm.)

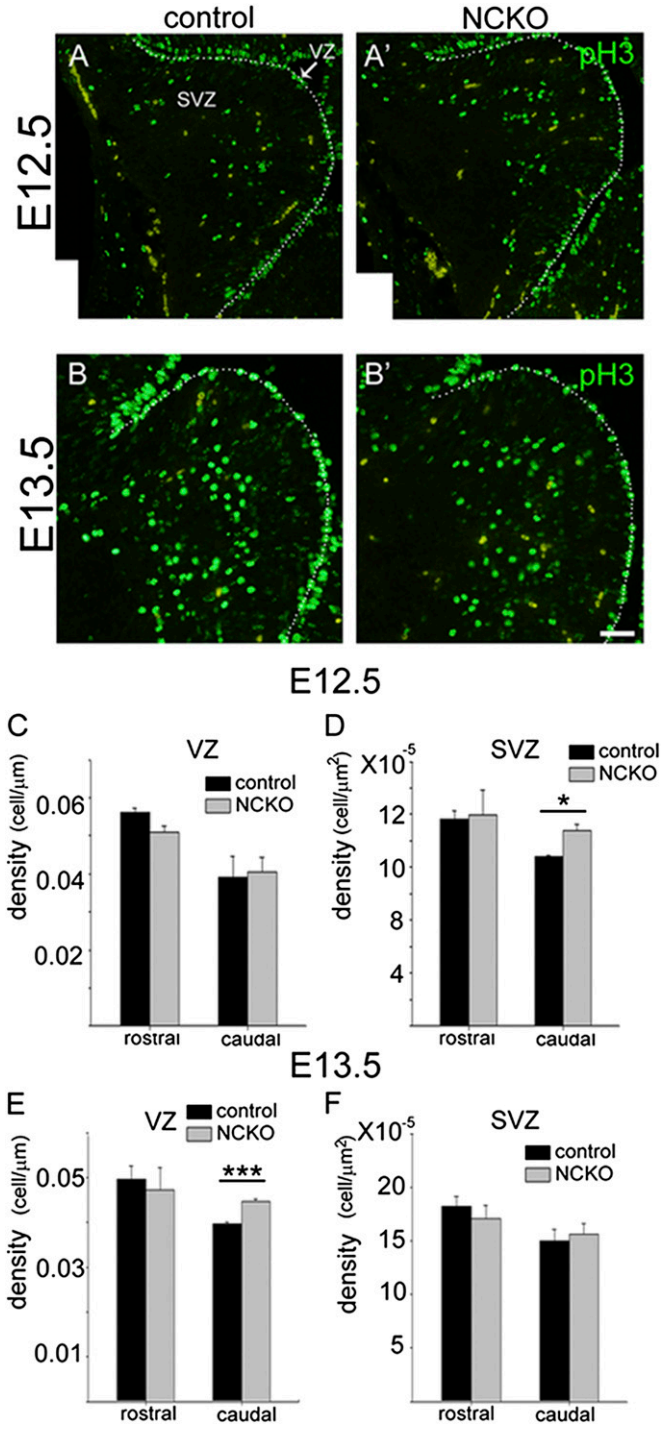

Fig. S7. Slight increases of phosphohistone 3$^+$ (pH3$^+$) mitotic cells in the germinal zones of Isl1 mutant striatal anlage. Immunostaining of pH3 shows that scattered pH3$^+$ mitotic cells are distributed in the ventricular zone (VZ, dashed lines along the lateral ventricle) and subventricular zone (SVZ) in control (*A* and *B*) and *Isl1* mutant (*A′* and *B′*) brains at E12.5 (*A* and *A′*) and E13.5 (*B* and *B′*). The density of pH3$^+$ cell number is not changed in rostral and caudal parts of E12.5 VZ (*A*, *A′* and *C*), but is slightly increased in the caudal parts of E12.5 SVZ (*A*, *A′*, and *D*) and E13.5 VZ (*B*, *B′*, and *E*) of mutant brains. $n = 3$. *$P < 0.05$; ***$P < 0.001$. (Scale bar: *A*–*B′*, 50 μm.)

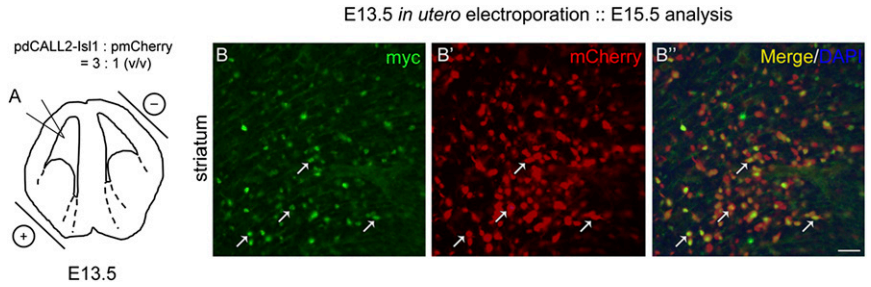

Fig. S8. Coelectroporation of pdCALL2-myc-*Isl1* and pCAG-mCherry plasmids into embryonic striatum by in utero electroporation. (*A*) pdCALL2-myc-*Isl1* plasmid was mixed with pCAG-mCherry plasmid at a ratio of 3:1 (vol/vol). The mixed plasmids were injected into the lateral ventricle of forebrains of E13.5 mouse embryos. The electrodes were held with angles of 45° and the anode facing the ventral telencephalons. (*B*) Electroporated brains were analyzed at E15.5 for the expression of pdCALL2-myc-*Isl1* by myc immunostaining. Merged images (*B*′′) show that almost all mCherry^{+} cells (*B*′, arrows) coexpress myc-Isl1 (*B*, arrows) in the electroporated striatum. (Scale bar: *B*–*B*′′, 50 μm.)